High-spin states in ^{210}Rn: The effect of the neutron holes on the four-proton configurations

A. R. Poletti*

Brookhaven National Laboratory and State University of New York at Stony Brook, Stony Brook, New York 11794

T. P. Sjoreen,† D. B. Fossan, U. Garg,‡ and A. Neskakis§

Physics Department, State University of New York at Stony Brook, Stony Brook, New York 11794

E. K. Warburton

Physics Department, Brookhaven National Laboratory, Upton, New York 11973

High-spin states in ^{210}Rn were observed with the aid of the ^{204}Pb(^{9}Be,$3n$)^{210}Rn reaction. γ-γ coincidence, excitation function, γ-ray angular distribution, and pulsed beam lifetime measurements were used to construct a decay scheme. Mean lives of four levels were deduced and multipolarities of γ-ray transitions and level spins were inferred.

INTRODUCTION

Until now nothing has been known of the structure of the nucleus ^{210}Rn. This nucleus with two neutron holes and four protons outside the ^{208}Pb closed shell nucleus is in a region where the shell model is known to give a very good description of the structure of the individual nuclei. As an example of just how well the shell model does work, let us consider the levels in ^{211}At which arise from the $(\pi h_{9/2})^3$ configuration. As de-Shalit and Talmi[1] show, the interaction energies of these levels are given by

$$\left\langle h_{9/2}{}^3 \nu J \left| \sum_{i<k}^{3} V_{ik} \right| h_{9/2}{}^3 \nu' J \right\rangle$$

$$= 3 \sum_{J_1} [h_{9/2}{}^3 \nu J \{ | h_{9/2}{}^2 (J_1) h_{9/2} J]$$

$$\times [h_{9/2}{}^3 \nu' J \{ | h_{9/2}{}^2 (J_1) h_{9/2} J]$$

$$\times \langle h_{9/2}{}^2 J_1 | V_{12} | h_{9/2}{}^2 J_1 \rangle \ , \qquad (1)$$

where the quantities $[\cdots \{ | \cdots]$ are the coefficients of fractional parentage[1] and the two-body interaction energies are obtained from the level energies (E_{J_1}) of the $(\pi h_{9/2})^2$ configuration[2] in ^{210}Po:

$$\langle h_{9/2}{}^2 J_1 | V_{12} | h_{9/2}{}^2 J_1 \rangle = {}^{210}\text{Po} + {}^{208}\text{Pb} - 2 \times {}^{209}\text{Bi} + E_{J_1}$$

$$= (1185.1 \pm 2.9) \text{ keV} + E_{J_1}. \qquad (2)$$

On the right-hand side of Eq. (2) the nuclear symbols stand for the ground state masses.[3] A similar relation connects level energies[4] and interaction energies in ^{211}At:

$$E_J = \left\langle h_{9/2}{}^3 \nu J \left| \sum_{i<k} V_{ik} \right| h_{9/2}{}^3 \nu J \right\rangle$$

$$- ({}^{211}\text{At} + 2 \times {}^{208}\text{Pb} - 3 \times {}^{209}\text{Bi}) \ ,$$

where from mass tables,[3] the term in brackets is $-(336 \pm 10)$ keV. The two-body interaction energies are given in Table I while Table II and Fig. 1(a) compare the energies calculated using Eq. (1) with the experimentally known members of the $(\pi h_{9/2})^3$ configuration in ^{211}At. The agreement is indeed excellent, especially for the high-spin states which are expected to be rather pure. The effect of two neutron holes on this three-particle spectrum can be examined by considering the nucleus ^{209}At. The influence of these neutron holes on the energies of the $(\pi h_{9/2})^3$ states will not be uniform and the energies of some of the levels will change much more than others.[5] The fact that this will occur can be seen by comparing the $(\pi h_{9/2})^2$ levels[6] in ^{208}Po with those[2] in ^{210}Po. In particular, in ^{208}Po the 2$^+$ state is at 687 keV whereas in ^{210}Po it is much higher in energy at 1181 keV. The energies of the other levels change by only a small amount. This can be understood in terms of the deformation of the core (now with two neutron holes) by the valence protons. The major effect of this is to cause a quadrupole distortion which lowers the energy of the 2$^+$ excitation. From Eq. (1) it is seen that the three-particle energies are a linear combination of the two-particle energies. Hence those $(\pi h_{9/2})^3$ levels in ^{209}At for which the coefficient of the 2$^+$ matrix element is large will be shifted by relatively large amounts. These are

TABLE I. Energies and interaction energies of the $(\pi h_{9/2})^2$ configurations in ^{210}Po and ^{208}Po.

| | Energies in keV | |
J	E_J	$\langle \pi h_{9/2}{}^2 J |V_{12}| \pi h_{9/2}{}^2 J \rangle$
	(a) ^{210}Po	
0	0	-1185 ± 3
2	1181	-4 ± 3
4	1427	242 ± 3
6	1473	288 ± 3
8	1557	372 ± 3
	(b) ^{208}Po	
0	0	-1154 ± 12
2	686	-467 ± 12
4	1347	193 ± 12
6	1524	370 ± 12
8	(1533)[a]	379 ± 13

[a] See Ref. 6.

TABLE II. Comparison between experimental and calculated energies of the $(\pi h_{9/2})^3$ configuration in ^{211}At.

| | Energies in keV | | |
2J	E_J^{expt}	E_J^{th}	$\Delta E = E^{\text{expt}} - E^{\text{th}}$
9	0	25 ± 10	-25 ± 10
7	866	834 ± 10	$+32 \pm 10$
5	947	960 ± 10	-13 ± 10
13	1067	1051 ± 10	$+16 \pm 10$
11	1123	1105 ± 10	$+18 \pm 10$
3	1116	1130 ± 10	-14 ± 10
9		1158 ± 10	
15	1270	1270 ± 10	0 ± 10
17	1321	1324 ± 10	-3 ± 10
21	1417	1423 ± 10	-7 ± 10

the $\frac{7}{2}$, $\frac{13}{2}$, $\frac{5}{2}$, and (to a lesser extent) the $\frac{11}{2}$ levels. Indeed, as can be seen from Fig. 1(b), of the levels experimentally determined, the $\frac{13}{2}$, $\frac{5}{2}$, and $\frac{11}{2}$, levels have all moved down significantly. The column labeled ^{209}At(^{208}Po) is the result of a calculation similar to that described by Eqs. (1) and (2) in which the two-particle interaction energies are taken from the spectrum of ^{208}Po. The core po-

larization effect should thus largely be accounted for. It can be seen by reference to Fig. 1(b) that the calculation largely reproduces the movements of the levels (from their positions in ^{211}At), especially the downward shift of the $\frac{11}{2}$, and $\frac{13}{2}$ levels.

A study, then, of the levels in ^{210}Rn and a comparison of their energies with those of the corresponding levels in ^{212}Rn can be expected to give much useful information on the way in which the presence of neutron holes influences the positions of the four-particle states. The positions and
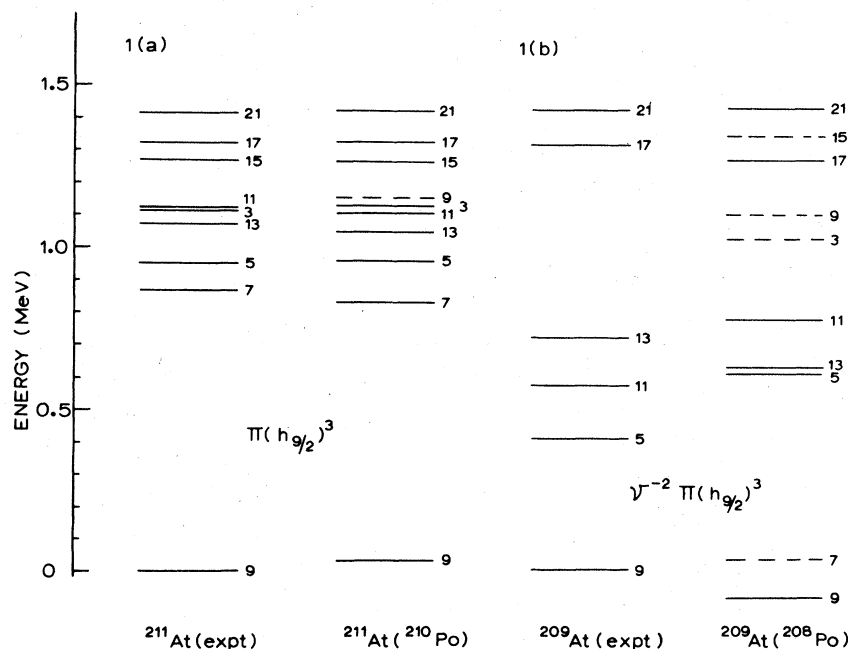

FIG. 1. (a) A comparison between the experimentally measured energies of the levels belonging th the $\pi(h_{9/2})^3$ configuration in ^{211}At with the energies calculated using the effective two-body matrix elements derived from the $\pi(h_{9/2})^2$ levels in ^{210}Po. (b) A similar comparison for the levels arising from the $\nu^{-2}\pi(h_{9/2})^3$ configuration in the nucleus ^{209}At. The dramatic lowering of the $\frac{13}{2}^-$ and $\frac{11}{2}^-$ levels which is due to the lower 2^+ excitation energy in ^{208}Po is evident. For both parts of the figure, levels are labeled by $2J$. Theoretically predicted but experimentally unobserved levels are dashed.

properties of the levels in ^{212}Rn have recently
been summarized by Horn *et al.*[7] As well as de-
termining the properties of high-lying core ex-
cited states, these authors also established the
properties of four-proton states belonging to the
$\pi h_{9/2}{}^4$, $\pi h_{9/2}{}^3 f_{7/2}$, $\pi h_{9/2}{}^3 i_{13/2}$, and $h_{9/2}{}^2 f_{7/2} i_{13/2}$ con-
figurations. In the present work we will be con-
sidering the effect of the neutron holes in ^{210}Rn on
levels belonging to the first three configurations.
These levels were excited by using the
^{204}Pb(^{9}Be, $3n)^{210}$Rn reaction at the Tandem Van de
Graaff Laboratory, Brookhaven National Labora-
tory. We will discuss the experimental results
obtained and interpret them in terms of the neu-
tron-hole influence on the four-proton states of
^{212}Rn.

EXPERIMENTAL

The properties of the yrast states in ^{210}Rn were
investigated with the aid of a number of standard
nuclear spectroscopic techniques:

   (i) γ-γ coincidence measurements using two
high resolution Ge(Li) spectrometers,

   (ii) excitation function measurements,

   (iii) γ-ray angular distribution measurements,

   (iv) pulsed beam lifetime measurements.

The γ-γ coincidence measurements were carried
out at a ^{9}Be beam energy of 50 MeV. A 10 mg cm^{-2}
^{204}Pb target which was self-supporting was bom-
barded with approximately 1.5 nA of ^{9}Be^{4+}. The
resulting γ rays were detected in two Ge(Li) spec-
trometers placed at angles of approximately ±110°.
The front face of each detector (approximately 5
cm from the target) was covered by 2.5 cm of
polyethylene to reduce the neutron dose and a
0.38 mm tantalum foil to attenuate the intense
x rays excited by the beam in the lead target. The
coincidences were event mode recorded (EMR) on
magnetic tape for subsequent playback. Analysis
of the coincident spectra enabled the level scheme
displayed in Fig. 2 to be constructed.

The excitation function measurement was needed
in order to verify the assignment to ^{210}Rn of the
γ rays observed in the coincidence experiment.
It was expected on theoretical grounds that the
$3n$ reaction leading to ^{210}Rn would peak at approxi-
mately 50 MeV while the $4n$ reaction (to ^{209}Rn)
would still be rising past 55 MeV. The measure-
ment was carried out using the same target as in
the previously described measurement and bom-
barding energies between 40 and 55 MeV. In addi-
tion, using 50 MeV, ^{9}Be^{4+}, and the same target,
the angular distributions of the ^{210}Rn γ rays were
measured. Finally, since the existence of at least
one isomeric level was suspected, a pulsed beam
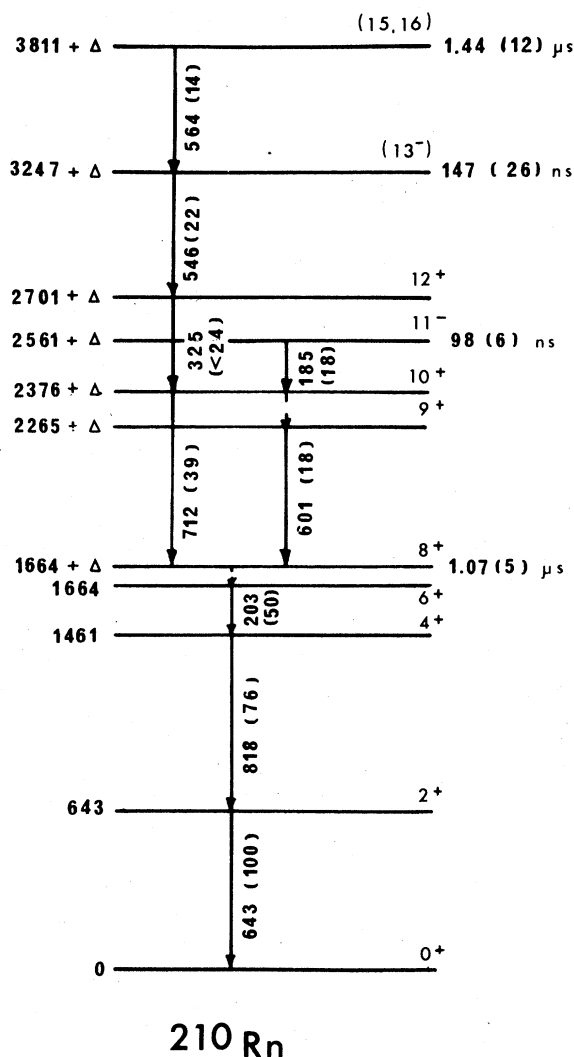experiment was undertaken. Again 50 MeV was

210 Rn

FIG. 2. The level scheme of ^{210}Rn deduced from the
present work. The 8$^+$ to 6$^+$ transition was not observed.
Its unknown energy (Δ keV) is expected to be of the order
of 30 keV by comparison with the properties of the simi-
lar transition in ^{212}Rn. The mean lives measured by us
are indicated on the right of the diagram. Relative ob-
served γ-ray intensities are given in brackets after the
transition energy. Spin assignments are those of the pre-
sent work.

chosen as the bombarding energy since this had
been shown to produce the optimum yield for the
gamma rays originating in ^{210}Rn. Beam pulses
with a pulse length of approximately 40 and 160 ns
were used. The pulses were separated in time by
1 and 4 μs, respectively.

RESULTS

An analysis of the γ-γ coincidence data revealed
that the γ rays, which from the excitation function
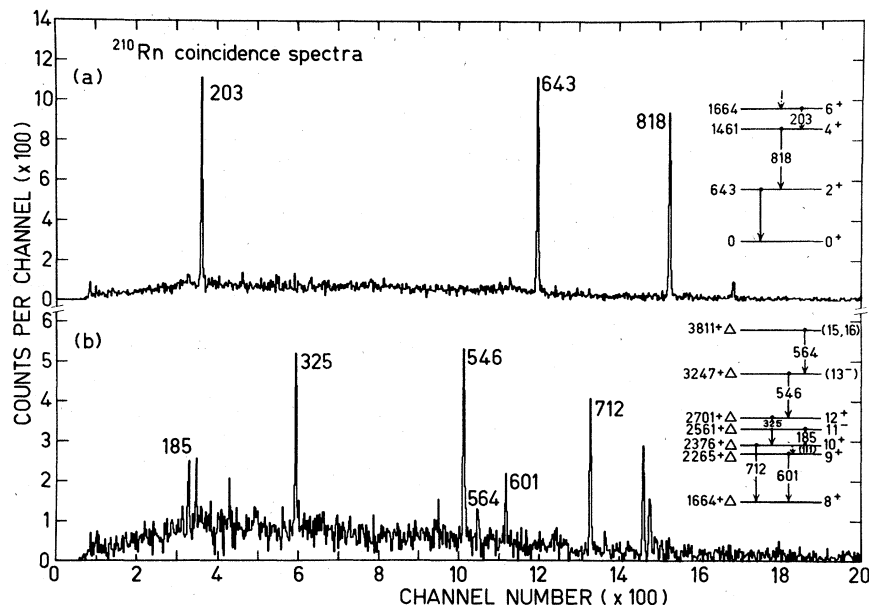measurement could be tentatively assigned to

FIG. 3. (a) The γ-ray spectrum obtained by adding together the spectra in coincidence with gates set on the photopeaks of the 203-, 818-, and 643-keV γ rays. (b) A similar spectrum illustrating the decay of the higher excited states (see text).

^{210}Rn, fell into two distinct families: The more intense family consisting of three γ rays of energies 203, 818, and 643 keV in cascade, while the other family consisted of γ rays of energies 564, 546, 712, 325, 185, and 601 keV. Composite coincidence spectra are shown in Fig. 3. To produce the final decay scheme we needed to draw on the results from all four investigations listed above. This synthesis allowed us to construct the decay scheme shown in Fig. 2. We identify the 203, 818, and 643 keV cascade with the deexcitation of a 6$^+$ state at 1664 keV. In placing an unobserved γ ray (energy Δ keV) just above the 1664-keV level and assigning it to an 8$^+$ to 6$^+$ transition, we are guided by the existence of an isomer between the two γ-ray families and by the established positions of the lowest 8$^+$ states in ^{212}Rn and the even Polonium isotopes. These states arise from the seniority two $(\pi h_{9/2})^2$ configuration. All reasonable short range interactions place the 8$^+$ level near and just above the 6$^+$ state. The nonobservation of this low energy γ ray is consistent too, with the high conversion coefficient expected. [The energy of the comparable transition in ^{212}Rn is 31 keV, for this energy $\alpha_k = 23.6$ for an $E2$ transition (Hager and Seltzer[8]).] Although coincidences between γ rays deexciting any of the three lower states and those placed above the 8$^+$ state were weak, they were clear enough to establish unequivocally the connection between these two sets of γ rays (and therefore the assignment of the states placed above the 8$^+$ level to ^{210}Rn). The excitation function

measurement is consistent with this assignment. It should be noted, however, that the 325 keV γ ray shows some coincidences with the 731-keV γ ray[5] in ^{209}Rn. It is assumed that there are γ rays of approximately 325 keV in both ^{209}Rn and ^{210}Rn.

The measured angular distributions are shown in Table III. They have been interpreted in terms of the heavy ion fusion-evaporation reaction model in which the fusion of the high energy ^{9}Be ions with the ^{204}Pb target leaves the compound nucleus highly

TABLE III. Angular distributions of gamma rays in ^{210}Rn excited in the ^{204}Pb(^{9}Be,$3n$)^{210}Rn reaction at 50 MeV. The distribution is expressed as intensity [1 $+a_2 P_2(\cos\theta) + a_4 P_4(\cos\theta)$], where the $P_L(\cos\theta)$ are Legendre polynomials and θ is measured with respect to the beam direction.

E_γ (keV)	Intensity [a]	a_2	a_4
185[b]	18	-0.10 ± 0.01	
203	50	0.13 ± 0.01	-0.03 ± 0.01
325[b,c]	24	0.10 ± 0.01	
546	22	-0.15 ± 0.02	-0.05 ± 0.03
564[b]	14	0.13 ± 0.03	
601	18	-0.60 ± 0.02	$+0.03 \pm 0.03$
643	100	0.11 ± 0.01	-0.02 ± 0.01
712	39	0.14 ± 0.01	-0.05 ± 0.02
818	76	0.15 ± 0.02	-0.05 ± 0.03

[a] Normalized to intensity of 643-keV 2$^+$–0$^+$ transition.
[b] For these transitions the a_4 coefficient was consistent with zero.
[c] Contaminated by a γ ray of similar energy in ^{209}Rn.

excited and in magnetic substates $|m_I| \leqslant \frac{3}{2}$. The subsequent evaporation of the low energy neutrons does little to alter this initial alignment. It is expected, therefore, that the states in ^{210}Rn will be initially populated in a highly aligned manner. Subsequent relaxation processes acting on long lived states would be expected to attenuate this initial alignment. The angular distribution of the three γ rays in the 203- 818-, and 643-keV cascade are consistent with their being quadrupole in nature, taking into account an attenuation of the characteristic distributions for the portion that is fed through the 8^+ isomer.

The 185-keV γ ray was seen to be in coincidence with both the 712- and 601-keV γ rays and no others placed higher in the decay scheme. The angular distribution and pulsed beam results argue that the 601-keV transition is a mixed $M1/E2$ transition while the 712-keV line is $E2$. An unobserved γ ray of 111 keV is hypothesized to explain the 185- and 601-keV coincidences. Nonobservation of this γ ray is consistent with an $M1$ conversion coefficient $\alpha_k \sim 8$ for $E = 111$ keV. If the 2265 +Δ- and 2376 +Δ-keV states are taken as yrast levels, the only spin assignments consistent with all observed properties are 9^+ and 10^+, respectively. The angular distributions of the 185- and 325-keV transitions are consistent with dipole and quadrupole transitions, respectively, while the 546-keV γ ray shows a distribution characteristic of a dipole transition. If the 185-keV transition is dipole then a consideration of the observed intensities (see Table III) and the $E1$ and $M1$ conversion coefficients for a γ ray of 185 keV (α_k is, respectively, 0.08 and 1.97) leads to the conclusion that this is an $E1$ transition. A spin-parity assignment of $J^\pi = 11^-$ to the 2561 +Δ-keV level is therefore consistent with all the data. Similarly, we assign 12^+ to the 2701 +Δ-keV level. The angular distribution of the 546-keV decay from the 3247 +Δ-keV level is consistent with an $E1$ transition. We suggest $J^\pi = (13^-)$. The 564-keV angular distribution was not well defined because of the weakness of this transition and was consistent with either a stretched quadrupole or octupole transition. This state could then have a spin of (15, 16).

Time spectra recorded using the pulsed beam enables us to measure the lifetimes of four states. That for the 564-keV γ ray showed no prompt peak (see Fig. 4). Analysis of the 4 μs data allowed us therefore to assign the measured mean life of (1440 ± 120) ns to the level at 3811 +Δ keV (see Table IV). Analysis of the time spectrum of the 546-keV γ ray was complicated by the occurrence of a prompt γ ray ~2 higher in energy. There was no conclusive evidence that the 546-keV γ ray had an associated prompt peak. There were,
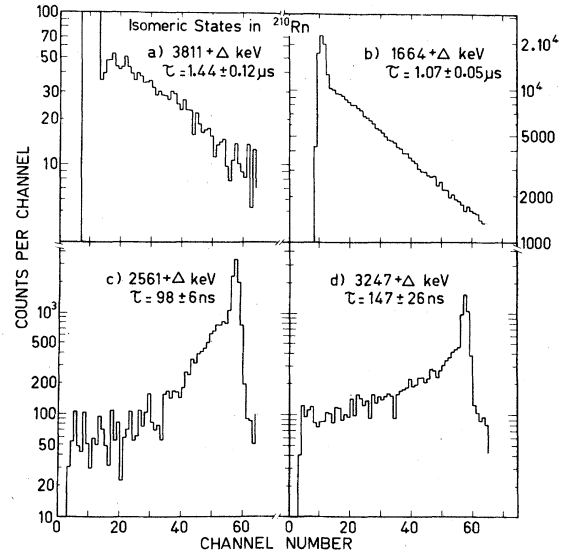

FIG. 4. Time spectra associated with the decay of the isomeric levels in ^{210}Rn investigated in this work: (a) 564-keV transition from the 3811+Δ-keV level. (b) A sum of the time spectra for the 203-, 643-, and 818-keV γ rays. This spectrum reflects the mean life of the 1664+Δ-keV level. For both of the above spectra the time calibration is 49.1 ns per channel. (c) 185-keV transition from the 2561+Δ-keV level. (d) 325-keV transition. This spectrum gives a measure of the mean life of the 3247+Δ-keV level. For these last two spectra the time calibration was 12.2 ns per channel.

however, two lifetimes associated with this line and with that at 325 keV. Fixing the mean life of the long lived component as 1440 ns (see above) enables us to extract from the 1 μs data the shorter mean like as (147 ± 26) ns. We assign this to the state at 3247 +Δ keV. The time spectrum of the 185-keV γ ray from the 1 μs data gave a clear single lifetime curve. We assign the measured mean life of (98.0 ± 6.2) ns to the state at (2561 ± Δ) keV. Analysis of the 4 μs time spectra associated with the 203-, 818-, and 643-keV γ rays gave

TABLE IV. Summary of lifetimes of excited states in ^{210}Rn using the ^{204}Pb(^{9}Be, $3n$)^{210}Rn reaction and a pulsed beam.

Level (keV)	Mean life (ns)	Comment
1644 +Δ	1070 ± 50	from time spectra of 203-, 644-, and 818-keV γ rays
2561 +Δ	98.0 ± 6.2	from time spectrum of 185-keV γ ray
3247 +Δ	147 ± 26	from time spectra of 325- and 546-keV γ rays
3811 +Δ	1440 ± 120	from time spectrum of 564-keV γ ray

(after allowing for the lifetimes of the states feeding the 8$^+$ level) a mean life of (1070 $\pm$ 50) ns for the 8$^+$ state which we place at 1664 $+\Delta$ keV.

DISCUSSION

In order to understand the level scheme obtained in the present work, it is necessary to consider the positions of the levels in ^{210}Rn which belong to the ν^{-2} $\pi(h_{9/2}{}^3f_{7/2})$ and ν^{-2} $\pi(h_{9/2}{}^3i_{13/2})$ configurations. The energies of the yrast levels belonging to the $\pi(h_{9/2}{}^4)$, $\pi(h_{9/2}{}^3f_{7/2})$, and $\pi(h_{9/2}{}^3i_{13/2})$ configurations have been calculated[7] for ^{212}Rn and show excellent agreement with the experimentally observed levels.[7] However, as the example of ^{209}At, discussed in the introduction showed, we can expect some of the levels of the four-particle configurations to be shifted quite substantially by the interaction with the two neutron holes so that a calculation which takes the effect of the neutron holes into account is needed. For the ν^{-2} $\pi(h_{9/2}{}^4)$ configuration we could do this directly by using the two-body matrix elements determined from the ^{208}Po spectrum (see Table I) and applying the standard shell model calculation (Ref. 1, Eq. 26.37). These calculated energies are compared with the experimental level scheme in Fig. 5. For the ν^{-2} $\pi(h_{9/2}{}^3f_{7/2})$, ν^{-2} $\pi(h_{9/2}{}^3i_{13/2})$ configuration, application again of the standard calculation (Ref. 1, Eq. 37.18) gave the levels shown on the right of Fig. 5. For these calculations we again took the two-body $h_{9/2}{}^2$ matrix element from the ^{208}Po spectrum. In addition, we needed the two-body $h_{9/2}f_{7/2}$ and $h_{9/2}i_{13/2}$ matrix elements. In principle these should be taken from the ^{208}Po spectrum but are not known at present. For both cases we expect the interaction energy to be much smaller and to have a smaller dependence on the coupled spin of the two-particle system than for the $h_{9/2}{}^3$ configuration because the particles involved are not in the same orbit. We therefore took these two-body matrix elements from the experimentally determined[2] $h_{9/2}f_{7/2}$ and $h_{9/2}i_{13/2}$ multiplets in ^{210}Po. The single particle energies of the $f_{7/2}$ and $i_{13/2}$ levels with respect to the $h_{9/2}$ ground state were taken as 897 and 1909 keV respectively from the spectrum of ^{209}Bi.

The results of these calculations are shown on the right-hand side of Fig. 5. The positions of the levels originating from the $h_{9/3}{}^3i_{13/2}$ configuration give a very good description of the 11$^-$ and (13$^-$) levels; however, then the lack of a fast E2 transition between them is surprising. It appears that the experimental 10$^+$ and 12$^+$ levels can be identified with the $(h_{9/2})^4$ levels although the somewhat higher theoretical energies may be an indication of configuration mixing with the levels of the same
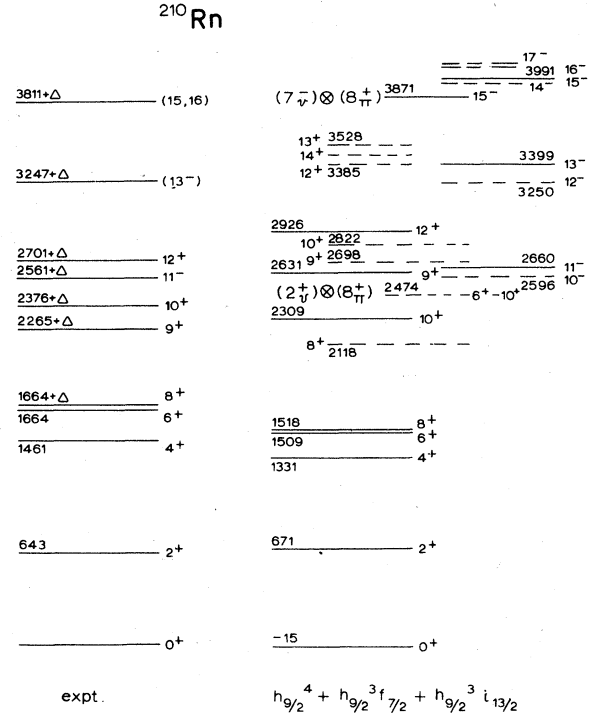

FIG. 5. A comparison between the levels in ^{210}Rn investigated in this work and some simple model calculations. Calculated levels are placed on the right directly above the respective configurations listed at the bottom. Dashed lines show levels theoretically predicted but experimentally unobserved. The positions of two levels arising from weak coupling of particle and hole excitations are indicated. Levels are labeled by energy in keV and spin-parity.

spin arising from $h_{9/2}{}^3f_{7/2}$. A 9$^+$ level below the 10$^+$ level is not predicted for any of the proton configurations, instead it probably arises from the weak coupling of the lowest (ν^{-2}), 2$^+$ state to the $\pi h_{9/2}{}^4$, 8$^+$ state. In this configuration the 9$^+$ state is expected to drop below the 10$^+$ state.[9] The highest level presents quite a puzzle. The $h_{9/2}{}^3i_{13/2}$ configuration is predicted to have levels of $J^\pi = 14^-$ to 17$^-$ in this region. The observed mean life of the 3811 $+\Delta$-keV level corresponds to an extremely inhibited M1 or E2 transition which seems unlikely for a transition between levels belonging to the same configuration, whereas M3 or E4 transitions demand enhancements which are not sensible. One possibility could be that this level represents the level obtained by weak coupling the 7$^-$ level in ^{206}Pb at 2200 keV to the 8$^+$ state at 1671 keV in ^{212}Rn to give a level at an excitation energy of about 3871 keV. The E2 decay of this level to the 13$^-$ state at 3247 $+\Delta$ keV could be expected to be strongly inhibited.

The above interpretation is obviously not unique. Instead of identifying the (13$^-$) level at 3247 $+\Delta$ keV

as $\pi(h_{9/2}{}^3 i_{13/2})$, it could arise from a hole excitation such as

$$\pi(h_{9/2}{}^4)_6 \otimes \nu(p_{1/2}{}^{-1} i_{13/2}{}^{-1})_7 .$$

The (15,16) level at $3811 + \Delta$ kev could similarly arise from

$$\pi(h_{9/2}{}^4)_6 \otimes \nu(f_{5/2}{}^{-1} i_{13/2}{}^{-1})_9 .$$

This interpretation could explain the lack of an observed transition between the (13^-) and 11^- state, but makes the extreme inhibition of the $3811 + \Delta \rightarrow 3247 + \Delta$ transition hard to understand. Appropriate admixtures of the above-mentioned configurations for the (13^-) and the (15, 16) levels could lead to a possible interpretation. More experimental data such as g-factor measurements are obviously needed together with more comprehensive calculations.

---

[1] A. de-Shalit and I. Talmi, *Nuclear Shell Theory* (Academic, New York, 1963).

[2] R. Tickle and J. Bardwick, Phys. Lett. 36B, 32 (1971).

[3] A. H. Wapstra and K. Bos, At. Data Nucl. Data Tables 19, 177 (1977).

[4] H. Ingwersen, W. Klinger, G. Schatz, and W. Witthuhn, Phys. Rev. C 11, 243 (1975) and references therein.

[5] T. P. Sjoreen, G. Schatz, S. K. Bhattacherjee, B. A. Brown, D. B. Fossan, and P. M. S. Lesser, Phys. Rev. C 14, 1023 (1976); I. Bergström, C. J. Herrlander, Th. Lindblad, V. Rahkonen, K.-G. Rensfelt, and K. Westerberg, Z. Phys. A273, 291 (1975); M. J. Martin, Nucl. Data Sheets 22, 545 (1977).

[6] K. Wikstrom, I. Bergström, J. Blomqvist, and C. J. Herrlander, Phys. Scr. 10, 292 (1974).

[7] D. Horn, O. Hausser, T. Faestermann, A. B. McDonald, T. K. Alexander, J. R. Beene, and C. J. Herrlander, Phys. Rev. Lett. 39, 389 (1977); in *Proceedings of the International Conference on Nuclear Structure, Tokyo, 1977*, edited by T. Marumori [J. Phys. Soc. Japan 44, (1978) Suppl. p. 605].

[8] R. S. Hager and E. C. Seltzer, Nucl. Data Sect. A 4, (1968).

[9] I. Bergström, J. Blomqvist, C. J. Herrlander, J. Hattula, O. Knuuttila, E. Liukkonen, and V. Rahkonen, Z. Phys. A287, 219 (1978).